

(Proposal to Jefferson Lab PAC-33)

$\vec{e}^-^2\text{H}$ Parity Violating Deep Inelastic Scattering (PVDIS) at CEBAF 6 GeV

A. Afanasev, P.E. Bosted, A. Camsonne, J.-P. Chen, E. Chudakov, A. Deur,
J.-O. Hansen, D.W. Higinbotham, D. Mack, R. Michaels (co-spokesperson) *,

A. Saha, A. Shahinyan, V. Sulkosky, and B. Wojtsekhowski

Thomas Jefferson National Accelerator Facility, Newport News, VA 23606, USA

D.S. Armstrong, T. Averett, J.M. Finn, K.A. Griffioen,, K. Grimm, and C. Perdrisat

College of William and Mary, Williamsburg, VA 23187, USA

J. Arrington, K. Hafidi, R. Holt, P.E. Reimer (co-spokesperson) †, and P. Solvignon

Physics Division, Argonne National Laboratory, Argonne, IL 60439, USA

E. Beise and H. Breuer

University of Maryland, College Park, MD 20742, USA

W. Bertozzi, S. Gilad, J. Huang, B. Moffit, P. Monaghan,

N. Muangma, A. Puckett, Y. Qiang, and X.-H. Zhan

Massachusetts Institute of Technology, Cambridge, MA 02139, USA

J.R. Calarco

University of New Hampshire, Durham, NH 03824, USA

G.D. Cates, N. Liyanage, V. Nelyubin, B.E. Norum, K. Paschke, J. Singh, R. Snyder,

R. Subedi, W.A. Tobias, K. Wang, and X.-C. Zheng (Contact and co-spokesperson) ‡

University of Virginia, Charlottesville, VA 22904, USA

P. Decowski

Smith College, Northampton, MA 01063

* email: rom@jlab.org

† email: reimer@anl.gov

‡ email: xiaochao@jlab.org

J. Erler

*Departamento de Física Teórica, Instituto de Física,
Universidad Nacional Autónoma de México, México D.F. 04510, México*

R. Holmes and P.A. Souder

Syracuse University, Syracuse, NY 13244, USA

T. Holmstrom

Randolph-Macon College, Ashland, VA 23005, USA

W. Korsch

University of Kentucky, Lexington, KY 40506, USA

K. Kumar and D. McNulty

University of Massachusetts, Amherst, MA 01003, USA

D.J. Margaziotis

California State University, Los Angeles, CA 90032, USA

P. Markowitz

Florida International University, Miami, FL 33199, USA

J. Roche

Ohio University, Athens, OH 45701, USA

B. Sawatzky

Temple University, Philadelphia, PA 19122, USA

N. Simicevic and S.P. Wells

Louisiana Tech University, Ruston, LA 71272, USA

S. Širca

University of Ljubljana, Slovenia

(the Hall A Collaboration)

(Dated: December 10, 2007)

The PDF file for the original proposal to PAC27 and this update can be downloaded from <http://hallaweb.jlab.org/experiment/E05-007/>

Abstract

We propose to measure the parity violating (PV) asymmetry A_d in \vec{e}^- - ^2H deep inelastic scattering (DIS) at $Q^2 = 1.11$ and 1.90 $(\text{GeV}/c)^2$ at $x \approx 0.3$. The combination of the two measurements will provide the first significant constraint on higher-twist (HT) effects in PVDIS at a level of $2.8\%/Q^2$. With HT effects thus measured, this experiment will constrain the poorly known effective weak coupling constant combination $(2C_{2u} - C_{2d})$. Assuming the Standard Model value for $(2C_{1u} - C_{1d})$ (tested separately by combining the Cs atomic parity violation (APV) experiments and the future QWeak experiment) the expected uncertainty upon completion of this 6 GeV measurement is $\Delta(2C_{2u} - C_{2d}) = \pm 0.033$, a factor of six improvement. The measurement will also allow the extraction of couplings C_{3q} from high energy μ -C DIS data. Precision measurements of all phenomenological couplings are essential to comprehensively search for possible physics beyond the Standard Model.

The constraint on HT effects in PVDIS provided by this experiment will provide an important guide for the future PVDIS program with the 12 GeV upgrade (using either the standard Hall C 12 GeV spectrometers or a dedicated large acceptance device) of which the ultimate goals are to study both the Electroweak Standard Model through extraction of the $2C_{2u} - C_{2d}$ and various exciting hadronic physics phenomena including the charge symmetry violation and the parton distribution ratio d/u at large x . The proposed measurement would also have immediate impact on other DIS analyzes, such as the extraction of $\sin^2 \theta_W$ from $\nu - N$ DIS (NuTeV) and the extraction of the strong coupling constant α_s from DIS data at low Q^2 .

The original proposal of this measurement (E05-007) was submitted to PAC 27 with a total beam time request of 46 days. This was divided into two phases: phase I (13 days including commissioning), and phase II (33 days). Phase I was approved by PAC 27 with an A- rating and is now going into the 3-year jeopardy. In this document we will provide updates to this proposal, including a review of the physics motivation, updates on the experimental setup, progress on the instrumentation development, updates on the systematic uncertainty estimation, beam time request, and collaboration status. We are submitting phase I here for jeopardy review, and we are requesting the full beam time (50 days). Since this is an update on progress since the PAC27 proposal,

several sections in the original proposal are not included in this update, but are still relevant to the experiment. These include 1.6 Exploring Physics Beyond the Standard Model, 2.1 Experimental Overview, 2.2 Beamline equipment, 2.3 Parity DAQ, 2.5 Luminosity Monitor, 2.6 Spectrometers, 2.8 Data Analysis, 3.1 Deadtime Correction, 3.2 Target Purity, Density Fluctuation and other False Asymmetries, 3.4 Pion background, 3.5 Pair Production Background, 3.7 Electroweak Radiative Corrections, 3.8 Experimental Uncertainties (Q^2 and the acceptance) and the method for kinematics optimization in 3.11.

Contents

1. Introduction - the Physics of PVDIS and Theoretical Updates	7
1.1. Parity Violating Electron Scattering	8
1.2. Weak Neutral Current Couplings and the Standard Model	10
2. Experimental and Theoretical Developments since PAC 27	12
2.1. Progress on the Weak Neutral Current Couplings at Low Q^2 and the Running of $\sin^2 \theta_W$	12
2.2. Updates on Hadronic Effects in PVDIS	15
2.2.1. Higher-Twist Effects	15
2.2.2. Charge Symmetry Violation (CSV)	16
3. Experimental Setup and Updates	21
3.1. Overview	21
3.2. Polarimetry	21
3.3. Progress on Target Cell Design	23
3.3.1. Target End Cap Contamination	24
3.3.2. Boiling Effect	25
3.3.3. Conclusion on Target Design	26
3.4. Update on DAQ	26
3.5. Overview of Instrumentation	29
4. Updates on Expected Uncertainties and Rate Estimation	30

4.1. Target End Cap Contamination	30
4.2. Electromagnetic (EM) Radiative Correction	31
4.3. Rescattering Background	33
4.4. Parton Distribution Functions and Ratio R	34
4.5. Higher Twists Effects	34
4.6. Charge Symmetry Violation (CSV)	35
4.7. Rate Estimation and Kinematics Optimization	35
4.8. Error Budget	35
5. Beam Time Request	39
6. Collaboration Status	40
7. Relation to other JLab Experiments and the 12 GeV Electroweak Physics Program	40
8. Summary	41
References	43

Update: PVDIS at 6 GeV

This is an update to proposal E05-007, Phase I of which was approved by PAC 27 and has come under the 3-year jeopardy. We will provide the scientific case, updates on the experimental setup and instrumentation development, and the collaboration status. The original proposal is supplementary to this update and is included in the PAC submission. In the original proposal, a total of 46 days was requested, divided into two phases. The first phase of 13 days was approved. Here we are requesting a total beam time of 50 days.

The original proposal as well as this update are available on the experiment's website: <http://hallaweb.jlab.org/experiment/E05-007/>

1. INTRODUCTION - THE PHYSICS OF PVDIS AND THEORETICAL UPDATES

With the advent of highly-polarized, high-current electron beams, parity violation measurements have become a standard tool for probing a variety of phenomena, including, for example, the Standard Model [1, 2], the role of strange quarks in the proton [3, 4, 5, 6, 7, 8], and the neutron distribution in nuclei [9]. These measurements have and will take place at accelerator facilities around the world. Recently, however, Jefferson Lab has become the notable host of many of these recent and future experiments. We propose a measurement of the asymmetry arising from parity violation (PV) in deep inelastic scattering (DIS) on a deuterium target, A_d , at $Q^2 = 1.1$ and 1.9 GeV to combined statistical and systematic uncertainty of 2.5%. These measurements will form the beginning of a PVDIS program that will continue to the 12 GeV program at JLab [10, 11]. While these measurements of A_d will take advantage of the high-quality CEBAF beam at JLab, they are not nearly as demanding as other completed or proposed PV measurements due to the relatively large asymmetry that will be measured, $A_d|_{Q^2=1.9 \text{ GeV}} \approx 160 \times 10^{-6}$.

The parity violating asymmetry in deep inelastic scattering (DIS) offers a unique window into two extremely interesting and exciting areas of physics. As will be shown in Sec. 1.1, this asymmetry is sensitive to the hadronic structure of the nucleon and to the Standard Model couplings C_{1u} , C_{1d} , C_{2u} and C_{2d} . The experiment proposed here will measure or limit the Q^2 dependence at fixed- x of A_d at low Q^2 to determine if higher twist terms play a significant role in the asymmetry. These measurements will be important for the future 12 GeV PVDIS program. If these measure-

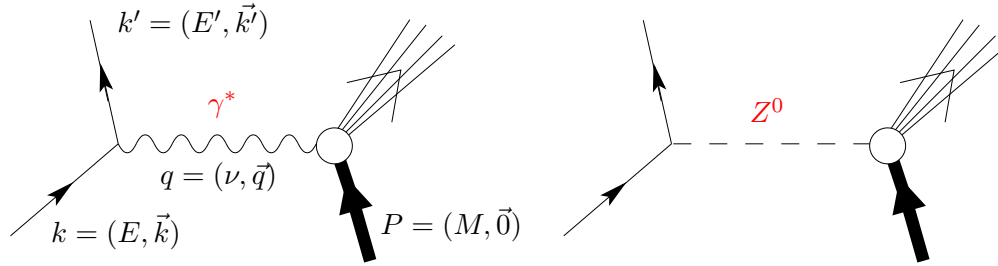


FIG. 1: Tree-level Feynman diagrams for electron scattering.

ments determine that higher twist contributions are sufficiently small then they may be used to constrain the C_2 coupling constants.

1.1. Parity Violating Electron Scattering

Electrons can scatter from nuclear target by exchanging either a virtual photon (γ^*) or a virtual Z^0 , as illustrated in Fig. 1. Until 1977, electrons had been used solely as an electromagnetic probe of the nucleon because the amplitude of weak neutral-current scattering at low energy is extremely small when compared with the electromagnetic amplitude. With the high-quality, intense, polarized electron beams now available, the weak neutral current can be accessed by measuring a parity-violating asymmetry that is proportional to the interference term between weak and electromagnetic scattering amplitudes [12].

For an electron scattering from a nuclear target, the scattering amplitude is the product of currents for the electron and the hadron, sandwiched around the photon and the Z^0 propagator \mathcal{M}_γ and \mathcal{M}_Z :

$$\mathcal{M}_\gamma = j_\mu \left(\frac{1}{q^2} \right) J^\mu; \quad \mathcal{M}_Z = j_\mu \left(\frac{1}{M_Z^2} \right) J^\mu. \quad (1)$$

With a longitudinally polarized electron beam, the cross sections for scattering right- and left-handed electrons off an unpolarized target is proportional to the square of the total amplitudes:

$$\sigma^r \propto (\mathcal{M}_\gamma + \mathcal{M}_Z^r)^2, \quad \sigma^l \propto (\mathcal{M}_\gamma + \mathcal{M}_Z^l)^2, \quad (2)$$

where \mathcal{M}_Z^r and \mathcal{M}_Z^l represent the amplitudes for incident right- and left-handed electrons, respec-

tively. The parity-violating asymmetry can be written as

$$A_{LR} \equiv \frac{\sigma^r - \sigma^l}{\sigma^r + \sigma^l} = \frac{(\mathcal{M}_\gamma + \mathcal{M}_Z^r)^2 - (\mathcal{M}_\gamma + \mathcal{M}_Z^l)^2}{(\mathcal{M}_\gamma + \mathcal{M}_Z^r)^2 + (\mathcal{M}_\gamma + \mathcal{M}_Z^l)^2} \approx \frac{\mathcal{M}_Z^r - \mathcal{M}_Z^l}{\mathcal{M}_\gamma}. \quad (3)$$

Measuring the parity-violating asymmetry allows one to access the weak neutral current in a ratio of amplitudes rather than the square of this ratio, greatly enhancing its relative contribution. A quick estimation of the asymmetry from the ratio of the propagators gives $A_{LR} \approx Q^2/M_Z^2 \approx 120$ ppm at $Q^2 = 1$ (GeV/c)².

In the specific case of DIS, the parity violating asymmetry for longitudinally polarized electrons scattering on an unpolarized deuteron target, A_d , is given by [12, 13]

$$A_d \equiv \frac{\sigma^r - \sigma^l}{\sigma^r + \sigma^l} = \left(\frac{3G_F Q^2}{\pi\alpha 2\sqrt{2}} \right) \frac{2C_{1u} - C_{1d}[1 + R_s(x)] + Y(2C_{2u} - C_{2d})R_v(x)}{5 + R_s(x)}, \quad (4)$$

where coefficients $C_{1,2u(d)}$ are given by Eq. (8-11) (see next page), $G_F = 1.166 \times 10^{-5}$ (GeV)⁻² is the Fermi weak interaction coupling constant and

$$Y = \frac{1 - (1 - y)^2}{1 + (1 - y)^2 - y^2 R / (1 + R)} \quad (5)$$

is a kinematic factor with $R \equiv \sigma_L/\sigma_T$, $y = \nu/E$ and $\nu = E - E'$ the energy loss of the incident electron. The ratios R_s and R_v are given by the quark distribution functions:

$$R_s(x) \equiv \frac{2[s(x) + \bar{s}(x)]}{u(x) + \bar{u}(x) + d(x) + \bar{d}(x)}$$

$$\text{and } R_v(x) \equiv \frac{u_V(x) + d_V(x)}{u(x) + \bar{u}(x) + d(x) + \bar{d}(x)}, \quad (6)$$

with $u_V(x)$ and $d_V(x)$ the valence quark distributions. Intrinsic charm can also be included in Eq. (4), introducing a similarly defined $R_c(x)$, but its effect is negligible at JLab energies. The lightest isoscaler target, Deuterium, is used in order to minimize the uncertainty due to parton distribution ratio $d(x)/u(x)$ while keeping the uncertainty due to nuclear effects small.

At relatively high x , $R_s \approx 0$ and $R_v \approx 1$ so that Eq. (4) reduces to

$$A_d = \left(\frac{3G_F Q^2}{\pi\alpha 2\sqrt{2}} \right) \left(\frac{1}{5} \right) [(2C_{1u} - C_{1d}) + Y(2C_{2u} - C_{2d})]. \quad (7)$$

In this limit, with $(2C_{1u} - C_{1d})$ experimentally determined by a variety of experiments including APV [14, 15, 16], PVES [17] and QWeak [2], it is clear that measurements at larger Y will have more sensitivity to $(2C_{2u} - C_{2d})$.

1.2. Weak Neutral Current Couplings and the Standard Model

The observation of a small parity violating asymmetry in DIS by SLAC experiment E122 played a key role in establishing the validity of the Standard Model [18, 19]. These results were consistent with $\sin^2 \theta_W \approx 1/4$, implying a tiny $V(\text{electron}) \times A(\text{quark})$ neutral current interaction. Subsequent PV measurements performed at both very low energy scales (atomic parity violation, or APV) as well as at the Z-pole are remarkably consistent with the results of this early DIS-parity measurement.

The Standard Model may be tested through the measurement of weak neutral current (WNC) interactions at $Q^2 \ll M_Z^2$. Pseudoscalar observables can be constructed from a product of vector- and axial-vector couplings. In electron-quark scattering with two active quark flavors, there are six possible couplings $C_{1,2,3u(d)}$. In the SM, these couplings may be expressed in terms of the weak mixing angle θ_W as:

$$C_{1u} = g_A^e g_V^u = -\frac{1}{2} + \frac{4}{3} \sin^2(\theta_W), \quad (8)$$

$$C_{1d} = g_A^e g_V^d = +\frac{1}{2} - \frac{2}{3} \sin^2(\theta_W), \quad (9)$$

$$C_{2u} = g_V^e g_A^u = -\frac{1}{2} + 2 \sin^2(\theta_W), \quad (10)$$

$$C_{2d} = g_V^e g_A^d = +\frac{1}{2} - 2 \sin^2(\theta_W), \quad (11)$$

$$C_{3u} = g_A^e g_A^u = -\frac{1}{2} \quad \text{and} \quad (12)$$

$$C_{3d} = g_A^e g_A^d = +\frac{1}{2}. \quad (13)$$

$C_{1u(d)}$ represents the axial Z-electron coupling g_A^e times the vector Z- $u(d)$ quark coupling $g_V^{u(d)}$, and the $C_{2u(d)}$ is the vector Z-electron coupling g_V^e times the axial Z- $u(d)$ quark coupling $g_A^{u(d)}$. Similarly, the C_{3q} are the products of axial-vector electron and quark couplings, and are therefore C-violating and parity conserving. Each of the C_{iq} terms might be sensitive to physics beyond the SM in different ways. Any deviation from Eq. (8-11) would indicate physics not contained in the Standard Model, placing the Standard Model as a piece of some larger framework [20]. Some of these possible new physics scenarios were discussed in Sec. 1.6 of the original proposal.

Among experiments (finished or planned) which will test the Standard Model and the search for new physics, some are purely leptonic (E158) and are not sensitive to new interactions involving quarks, some are semi-leptonic (APV, QWeak) but can only access the weak couplings C_{1q} . In

TABLE I: Existing data on P - or C -violating coefficients C_{iq} compiled in Ref. [23] (except where noted). For each measured result, the statistical, systematic and theoretical uncertainties are combined in quadrature. For some of the quantities listed here, global analysis gives slightly different values, please see Ref. [22] for the most recent updates.

facility	process	$\langle Q^2 \rangle$ (GeV/c) ²	C_{iq} combination	result	SM value
SLAC [18, 19]	e^- D DIS	1.39	$2C_{1u} - C_{1d}$	-0.90 ± 0.17	-0.7185
*[-0.10in]		1.39	$2C_{2u} - C_{2d}$	$+0.62 \pm 0.81$	-0.0983
CERN	μ^\pm C DIS	34	$0.66(2C_{2u} - C_{2d})$ $+ 2C_{3u} - C_{3d}$	$+1.80 \pm 0.83$	+1.4351
CERN	μ^\pm C DIS	66	$0.81(2C_{2u} - C_{2d})$ $+ 2C_{3u} - C_{3d}$	$+1.53 \pm 0.45$	+1.4204
Mainz	e^- Be QE	0.20	$2.68C_{1u} - 0.64C_{1d}$ $+ 2.16C_{2u} - 2.00C_{2d}$	-0.94 ± 0.21	-0.8544
Bates [24]	e^- C elastic	0.0225	$C_{1u} + C_{1d}$	0.138 ± 0.034	+0.1528
Bates [25]	e^- D QE	0.1	$C_{2u} - C_{2d}$	-0.042 ± 0.057	-0.0624
Bates [25]	e^- D QE	0.04	$C_{2u} - C_{2d}$	-0.12 ± 0.074	-0.0624
JLab [2]	e^-p elastic	0.03	$2C_{1u} + C_{1d}$	approved	+0.0357
--	¹³³ Cs APV [14]	0	$-376C_{1u} - 422C_{1d}$	-72.69 ± 0.48	-73.16
--	²⁰⁵ Tl APV [15]	0	$-572C_{1u} - 658C_{1d}$	-116.6 ± 3.7	-116.8
Combined Fit PVES Data [17, 26]	e^- A	low	$C_{1u} + C_{1d}$	0.1358 ± 0.0326	0.1528
			$C_{1u} - C_{1d}$	-0.4659 ± 0.0835	0.5297
			$C_{2u} + C_{2d}$	-0.2063 ± 0.5659	-0.0095
			$C_{2u} - C_{2d}$	-0.0762 ± 0.0437	-0.0621

contrast to C_{1q} , the weak coupling C_{2q} and C_{3q} are poorly known. Table I summarizes the current knowledge of C_{iq} [21]. From existing experimental data, $2C_{2u} - C_{2d} = 0.254 \pm 0.193$ [22]¹. This constraint is poor and must be improved in order to enhance sensitivity to many possible extensions

¹ This number is based on the 2006 Review of Particle Properties [22], including correlations. The PAC 27 proposal used an earlier PDG value with a corresponding uncertainty of $\Delta(2C_{2u} - C_{2d}) = \pm 0.24$, slightly larger than the uncertainty here.

of the SM, such as quark compositeness and new gauge bosons. $e\text{--}^2\text{H}$ PV DIS can provide precise data on $2C_{2u} - C_{2d}$ which are not accessible through other processes. We expect to improve the uncertainty on $2C_{2u} - C_{2d}$ by a factor of six.

The eD DIS experiment proposed here will also impact our knowledge of the C_{3q} . The only available measurement sensitive to these is the CERN $\mu^\pm\text{C}$ DIS experiment [27] (see Tab. I). The combination $2C_{3u} - C_{3d}$ is only known to about 50% precision, which is partly due to a large global correlation coefficient of 0.82 with the C_{1q} and C_{2q} . The experiment proposed here would reduce this correlation to $< 6\%$, essentially decoupling the CERN combination, $2C_{3u} - C_{3d}$, and reducing its uncertainty by more than 40%.

2. EXPERIMENTAL AND THEORETICAL DEVELOPMENTS SINCE PAC 27

Since these measurements were proposed to PAC 27, there have been several new measurements and analyses of data that provide greater insight into the PVDIS asymmetry, the C_{iq} couplings and the running of $\sin^2 \theta_W$. Also reviewed are possible hadronic contributions to the PVDIS asymmetry, including information from recent parton distribution fits studying charge symmetry violation. These are discussed below.

2.1. Progress on the Weak Neutral Current Couplings at Low Q^2 and the Running of $\sin^2 \theta_W$

The most recent data on the semi-leptonic weak neutral current couplings is summarized in Tab. I. The notable addition to this table is a recent analysis by R. Young *et al.* [17, 26] that considered data from several recent parity violating electron scattering (PVES) experiments [3, 4, 5, 6, 7, 8, 28, 29] as part of a fit for the C_{iq} coefficients, see Fig. 2. In addition to fitting the PVES alone, the data were included in a more global fit of all relevant data. As can be seen from Fig. 2, this new fit provides a constraint in the $C_{1u} - C_{1d}$ vs. $C_{1u} + C_{1d}$ plane that is orthogonal to the Cs Atomic Parity Violation data, greatly reducing the available phase space. In the $C_{2u} - C_{2d}$ vs. $C_{2u} + C_{2d}$ plane the reduction in phase space is much less significant. Expected results on the C_{2q} from the proposed measurements are also shown.

Within the framework of the Standard Model, all of the C_{iq} coefficients are proportional to $\sin^2 \theta_W$, as given in Eqs. (8-13). The running of $\sin^2 \theta_W$ as a function of Q^2 is now reasonably established, as is shown in Fig. 3. Since the earlier proposal, the SLAC E-158 Møller experiment

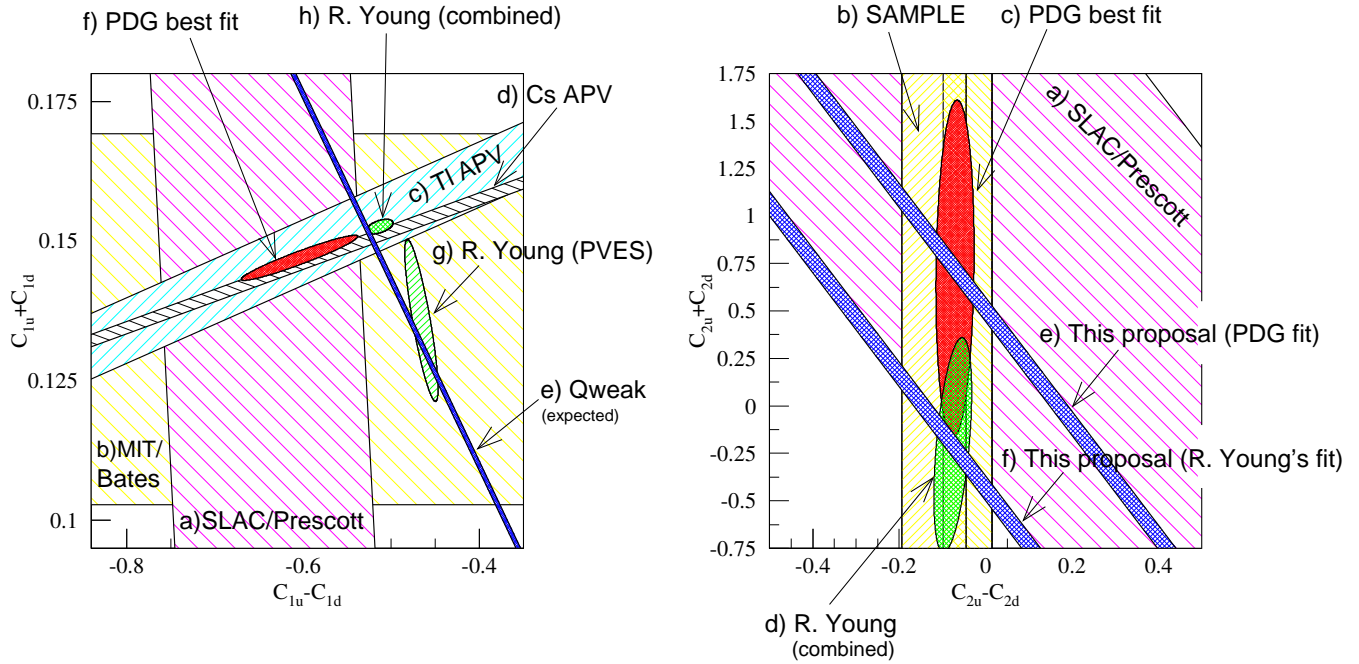


FIG. 2: The current experimental knowledge of the effective couplings C_{1u} , C_{1d} (left), C_{2u} and C_{2d} (right). Shown in the $C_{1u} + C_{1d}$ vs. $C_{1u} - C_{1d}$ plot are a) the SLAC A_d measurement [18, 19] (magenta band); b) elastic scattering data from MIT Bates [24] (yellow hatched region); c) TI APV [15, 16] (diagonal cyan hatched band); d) Cs APV [14, 16] (black hatched band); e) the expected precision of the QWeak experiment [2] plotted at the Standard Model values [22] (blue cross hatched band); f) the PDG's best fit [22] (red ellipse); g) R. Young *et al.* fit to PVES data [17, 26] (green single hatched ellipse); and h) R. Young *et al.* fit to PVES and APV data combined [17, 26] (small green cross hatched ellipse). Shown in the $C_{2u} + C_{2d}$ vs. $C_{2u} - C_{2d}$ plot are a) the SLAC A_d measurement [18, 19] (magenta band); b) the SAMPLE experiment interpreted in terms of C_{2q} coefficients [25] (yellow bands); c) the PDG's best fit [22] (red ellipse); d) R. Young *et al.* fit to all data combined [17, 26] (green cross hatched ellipse); and e-f) the expected uncertainty from the proposed measurement, plotted at the best fit values from the PDG best fit (upper blue cross hatched band) and at the R. Young *et al.* [17, 26] best fit values (lower blue cross hatched band). Note that the Young fit includes much of the same data as the PDG fit, so that they should not be considered as independent. All limits are at one standard deviation. Finally, several measurement listed in Tab. I which correlate the C_1 and C_2 coefficients are not shown; although these data are included in the PDG fits.

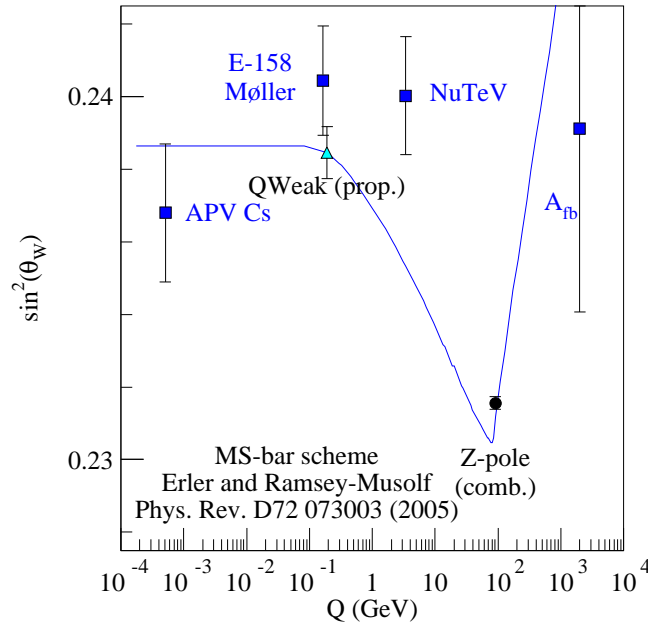


FIG. 3: The curve illustrates the running of $\sin^2 \theta_W$ [21] and existing measurements from Cs APV [14], Fermilab NuTeV [31], SLAC E185 Møller [1, 30] and the expected uncertainty of the JLab QWeak experiment [2].

has completed its analysis and these results are in statistical agreement with the Standard Model [1, 30].

The NuTeV anomaly [31], an apparent three standard deviation difference with the prediction based on the Standard Model, still exists. A difference between $s(x)$ and $\bar{s}(x)$ could have accounted for some of this difference. A recent analysis next-to-leading order analysis of dimuon events in ν DIS by the NuTeV experiment has found an asymmetry between s and \bar{s} but with only a 1.6 standard deviation significance. Even assuming this asymmetry to be correct and not a statistical fluctuation, its magnitude is not enough for it alone to explain the NuTeV anomaly [32]. Higher twist terms may also contribute significantly to the NuTeV result [33]. The proposed PVDIS measurements at $Q^2 = 1.0$ and 1.9 GeV^2 can be used to tightly constrain HT contributions to the NuTeV anomaly.

2.2. Updates on Hadronic Effects in PVDIS

2.2.1. Higher-Twist Effects

At the kinematics of the proposed measurements, higher-twist effects (HT) may contribute to the measured value of A_d . Higher-twist effects refer to the fact that the color interactions between the quarks become stronger at low Q^2 and the process cannot be described by the leading twist diagram of Fig. 1. For electro-magnetic scattering processes, these interactions introduce a scaling violation to the structure functions in the low Q^2 region [below 1 (GeV/c)^2] that is stronger than the $\ln(Q^2)$ -dependence of the DGLAP equations of pQCD. For PV $\vec{e}^{-2}\text{H}$ scattering, HT effects start from twist-four terms which diminish as $1/Q^2$.

The theory for HT effects is not well established. Most of the knowledge for HT is from data on DIS structure functions F_1 , F_2 , g_1 and g_2 . When determining the HT effects from these data, the leading twist (LT) contribution often cannot be subtracted cleanly because of the uncertainty due to the cutoff in summing the α_s series, and the uncertainty in α_s itself in the low Q^2 region. The first parameterization of the HT coefficient C_{HT} , extracted from F_2 data using $F_2^{data} = F_2^{LT}(1 + C_{HT}/Q^2)$ with Q^2 in $(\text{GeV}/c)^2$, showed sizable effect for all x values that increases dramatically at higher x [34]. In this extraction the pQCD Q^2 -evolution was removed up to Next-Leading-Order (NLO). The latest fit to the HT coefficient, however, shows that the effect for $0.1 < x < 0.4$ diminishes quickly to $< 1\%/Q^2$ as higher order terms (NNLO and NNNLO) are included when evaluating the leading-twist term [35].

There is almost no data on the HT contribution to PV observables. Theoretically, estimates of the twist-four corrections to the asymmetry in $\vec{e}^{-2}\text{H}$ DIS have been carried out in various models. In a work by Castorina and Mulders [36], the HT contribution to the $\vec{e}^{-2}\text{H}$ asymmetry was evaluated in the MIT bag model and was found to be 0.3% at $Q^2 = 1.0 \text{ (GeV}/c)^2$. In a similar work by Fajfer and Oakes where in addition the deuteron matrix element of the operators was used, it was found that the higher-twist effects decrease the value of $\sin^2 \theta_W$ by less than 1% [37]. This corresponds to $< 2\%/Q^2$ contribution to the PVDIS asymmetry.

The second approach to estimate HT correction to PVDIS is based on experimental data on C_{HT} and the assumption that the HT effects partly cancel in the numerator and the denominator of the asymmetry. Presumably, the higher twist dynamics is the same for the γ^* and Z_0 exchange processes in PVDIS as that for F_2 , hence cancel in the asymmetry. One possible effect that does

not cancel comes from the different coupling strength of the EM and weak interactions in the interference term, which is proportional to the EM and weak charges, respectively. Quantitative calculations for the HT correction to A_d were performed in the QCD LO, NLO and NNLO framework [38]. Parameterization of C_{HT} by Virchaux and Milsztajn [34] was used as an input. The results show the HT correction to A_d is at level of $1\%/Q^2$ for $0.1 < x < 0.3$ in NLO or higher order analysis.

The HT corrections to PVDIS and to NuTeV may be connected. In a model by Gluck and Reya [33], it was shown that although the NuTeV measurement was performed at $\langle Q^2 \rangle = 20 \text{ (GeV}/c)^2$, the HT contribution to the typically measured Paschos-Wolfenstein (P-W) ratio could be of the same magnitude as that to the PVDIS observable at $Q^2 \approx 2 \text{ (GeV}/c)^2$. Because the P-W ratio measured by NuTeV is 2.5% lower than the SM value, a 2.5% HT correction to this ratio will remove the 3σ anomaly. According to this model, a 2.5% contribution to the P-W ratio at $Q^2 = 20 \text{ (GeV}/c)^2$ implies a $\approx 4\%$ HT contribution to our high Q^2 measurement and a $\approx 8\%$ contribution to our low Q^2 measurement. Since the asymmetry A_d will be measured to 2.11% at the low Q^2 point, this effect will be observable if the HT is indeed the dominant reason of the NuTeV anomaly. Therefore, depending on the future experimental situation and the outcome of the experiment proposed here, one will possibly gain a better understanding of the NuTeV anomaly and validate this model of HT effects.

Overall, most theories predict that the HT contribution to A_d is at the $1\%/Q^2$ level. If so, the effect at our high Q^2 point will be about $1/5$ of the statistical error and will not be significant. However, there has been no experimental proof of these theories. Therefore A_d will also be measured at $Q^2 = 1.11 \text{ (GeV}/c)^2$. If the HT contribution is statistically significant at the high Q^2 measurement, it will show up more significantly at this low Q^2 . This first observation of the HT effect in PV asymmetries will also provide crucial input to the future PVDIS program at 12 GeV, and may help to explain the NuTeV anomaly.

2.2.2. Charge Symmetry Violation (CSV)

Charge symmetry is the equivalence between $u(d)$ quark distributions in the proton and $d(u)$ quarks in the neutron. Most low energy tests of charge symmetry found it is good to at least 1% level [39] so it is usually assumed to be justified in discussions of strong interactions. However,

charge symmetry is not strictly true since the constituent mass of the d quark is heavier than the u quark. Recent progress have been made in both understanding QED effects in the DGLAP evolution which contribute to charge symmetry violation (CSV) and to global fits of to data that allow for CSV.

The CSV distributions are defined as [40]

$$\delta u(x) = u^p(x) - d^n(x) , \quad (14)$$

$$\delta d(x) = d^p(x) - u^n(x) , \quad (15)$$

where the superscripts p and n refer to the proton and neutron, respectively. Eq. (14) is usually referred to as the “majority” CSV term and Eq. (15) is the “minority” CSV term. The relations for CSV in anti-quark distributions are analogous. Taking into account the CSV effect, Eq. (4) becomes

$$A_d = \left(\frac{3G_F Q^2}{\pi\alpha 2\sqrt{2}} \right) \quad (16)$$

$$\times \frac{2C_{1u} [1 + R_c(x) - R_{\delta d}] - C_{1d} [1 + R_s(x) - R_{\delta u} - R_{\delta s}] + Y (2C_{2u} - C_{2d}) \left[R_v(x) - \frac{R_{\delta u_v}}{3} - \frac{2R_{\delta d_v}}{3} \right]}{5 + R_s(x) + 4R_c(x) - R_{\delta u} - 4R_{\delta d} - R_{\delta s}}$$

where $R_{\delta q}$ and $R_{\delta q_v}$ are defined as

$$\begin{aligned} R_{\delta u} &= \frac{\delta u(x) + \delta \bar{u}(x)}{u(x) + \bar{u}(x) + d(x) + \bar{d}(x)} , \\ R_{\delta d} &= \frac{\delta d(x) + \delta \bar{d}(x)}{u(x) + \bar{u}(x) + d(x) + \bar{d}(x)} , \\ R_{\delta u_v} &= \frac{\delta u_v(x)}{u(x) + \bar{u}(x) + d(x) + \bar{d}(x)} \\ \text{and } R_{\delta d_v} &= \frac{\delta d_v(x)}{u(x) + \bar{u}(x) + d(x) + \bar{d}(x)} . \end{aligned} \quad (17)$$

with $u(x)$, $d(x)$, $\bar{u}(x)$ and $\bar{d}(x)$ in the denominator PDF values for the proton.

One source of CSV is the Coulomb splitting effect. Until recently, the QED splitting effect had not been included in parton distributions fits. This effect arises from different DGLAP evolution of the u and d quark parton distributions. These splitting functions have now been calculated in NNLO [41, 42] and they are included in parton distribution fits [43]. Figure 4 shows the size of QED-splitting CSV for $Q^2 = 1.25 \text{ (GeV/c)}^2$ and $Q^2 = 2.0 \text{ (GeV/c)}^2$, respectively and are tabulated in Tab. II. It should be emphasized that this QED effect is not an uncertainty in the

parton distributions, but rather an effect of the DGLAP evolution that, while previously ignored, is now correctly accounted for in the parton distributions. Hence CSV from QED splitting will not contribute to the overall uncertainty in the measurement.

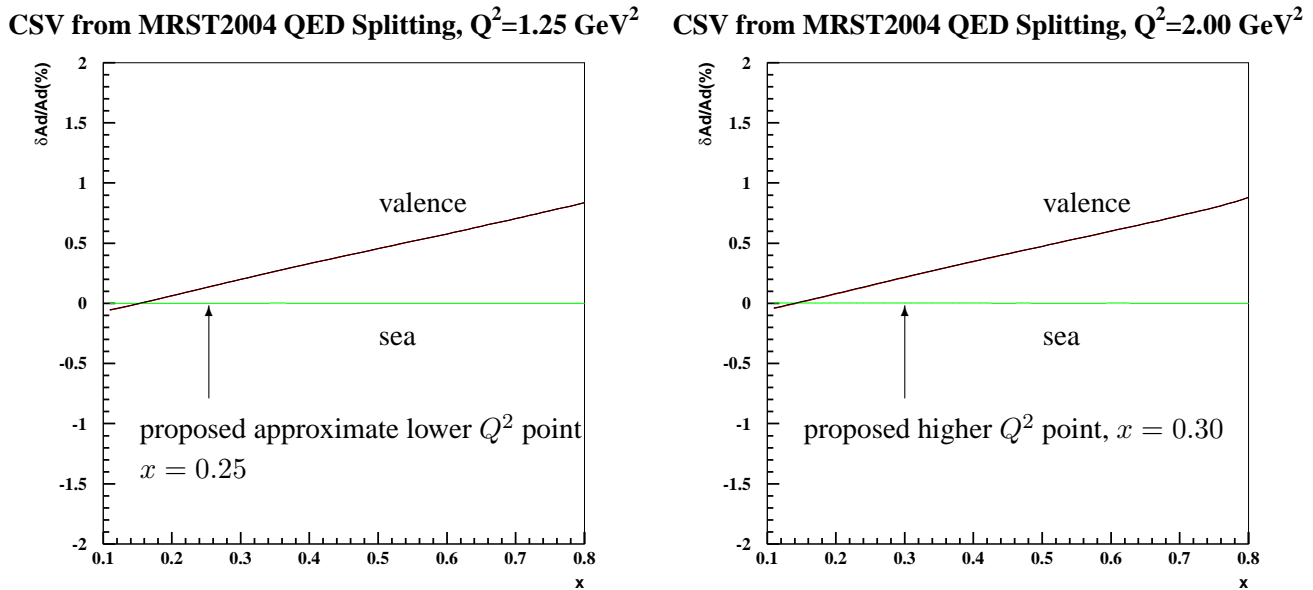


FIG. 4: Effect on A_d from QED-splitting CSV as functions of x at 6 GeV for $Q^2 = 1.25 (\text{GeV}/c)^2$ (left) and $Q^2 = 2.0 (\text{GeV}/c)^2$ (right). For each Q^2 , effects from valence (black) and sea quark CSV (green) are shown separately. The total QED-splitting CSV is clearly dominated by the valence quarks. Kinematics of the proposed measurement are shown by arrows. There is a slight difference in the Q^2 of the left plot and the proposed value; however, by comparing the two Q^2 values we can see that calculations at $Q^2 = 1.25$ would provide an upper limit on the value at $Q^2 = 1.11 (\text{GeV}/c)^2$.

In the original proposal we have used the MIT bag model to calculate CSV distributions for the valence [44] and the sea quarks, and found quite small CSV contribution to A_d . We also used the MRST2003 PDF sets which allowed for CSV effects in the fits, and found that CSV for valence quarks is smaller, but the CSV for sea quarks is larger than the MIT bag model predictions.

Prior to the inclusion of QED CSV, the MRST group looked for empirical evidence for CSV

TABLE II: Magnitude of the QED CSV effects on A_d . These numbers represent the contribution of the known correction to the asymmetry due to QED CSV in the parton distributions. These effects are now accounted for in the parton distributions. The lower Q^2 value given here is limited by the MRST parameterization and is slightly different from the proposed value, $Q^2 = 1.11 \text{ (GeV}/c)^2$. However it should provide an upper limit on the effects at this proposed kinematics.

Source	$Q^2 = 1.25 \text{ (GeV}/c)^2$	$Q^2 = 1.90 \text{ (GeV}/c)^2$
valence	0.135%	0.215%
sea	0.001%	0.002%
total	0.136%	0.217%

through a parton distribution fit [35] that allowed for the CSV parameterized as

$$u_V^n(x) = d_V^p(x) + \kappa f(x) \quad (18)$$

$$d_V^n(x) = u_V^p(x) + \kappa f(x) \quad (19)$$

$$u_{\text{sea}}^n(x) = d_{\text{sea}}^p(x) (1 + \delta) \quad (20)$$

$$d_{\text{sea}}^n(x) = u_{\text{sea}}^p(x) (1 + \delta) \quad (21)$$

Based on these parameterizations, the global fit found that data favored a slight CSV in both the valence and sea quark distributions. For valence quarks the nominal value is $\kappa = -0.20$ with a 90% C.L. range of $\kappa = (-0.80, 0.65)$. For sea quarks the nominal value is $\delta = 0.08$ with a 90% C.L. range of $\delta = (-0.08, 0.18)$. These results are summarized in Fig. 5 for A_d . Note that this fit includes both the calculable QED CSV as well as any anomalous, hadronic CSV.

From Figs. 4 one can see that the QED-splitting CSV is overall much smaller than the proposed statistical uncertainty (2.1% upon full completion). QED CSV is now included in parton distribution fits. From Fig. 5, the global fit looking for *any* CSV from any source found that CSV is likely to be small; however, the 90% C.L. range indicate that this effect could only be half of the proposed statistical uncertainty. Calculations for the hadronic CSV effects at the exact proposed kinematics will be given in Section 4.8.

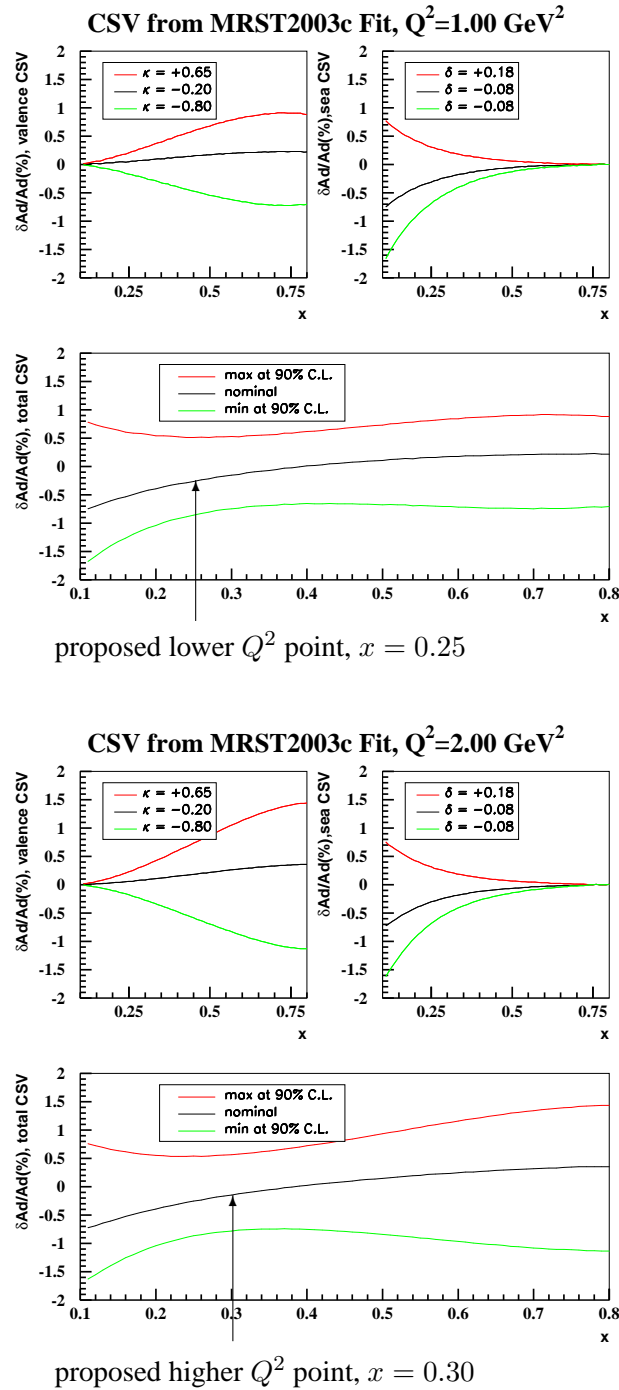


FIG. 5: Effect on A_d from CSV as parameterized by MRST [35] as functions of x at 6 GeV for $Q^2 = 1.0 \text{ (GeV/c)}^2$ (top) and $Q^2 = 2.0 \text{ (GeV/c)}^2$ (bottom), respectively. For each Q^2 , effects from the valence and the sea quarks' CSV are shown separately (top left and top right), then the total CSV effects is shown in the bottom. The nominal values (black or central curve) are shown as well as the 90% C.L. values (red and green, or higher and lower curves, respectively). Kinematics of the proposed measurement are shown by arrows. Note that these results include both the calculable QED CSV as well as any anomalous hadronic CSV.

3. EXPERIMENTAL SETUP AND UPDATES

3.1. Overview

The experimental setup remains the same as the original proposal. The floor plan for Hall A is shown in Fig. 3.1. We use an $85 \mu\text{A}$ polarized beam and a 25 cm liquid deuterium target. The scattered electrons are detected by the two standard Hall A High Resolution Spectrometers (HRS). A fast Data Acquisition (DAQ) system will be built to accommodate a rate as high as 1 MHz from each HRS. A Luminosity Monitor (Lumi) is located downstream on the beam-line to monitor the helicity-dependent target boiling effect and possible false asymmetries to a 10^{-7} level.

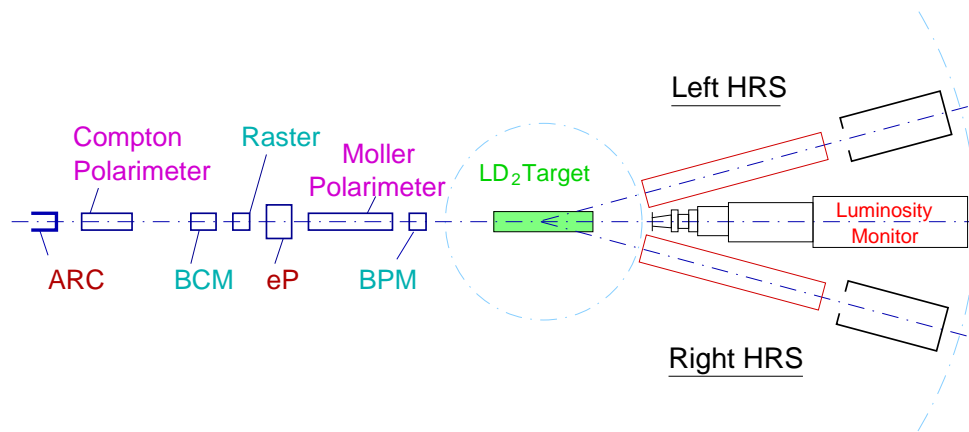


FIG. 6: Hall A floor plan for the proposed measurement.

The instrument needed by the PVDIS measurement was described in details in Section 2 of the original proposal. Sections in the original proposal that will not be included in this update are: 2.2 Beamline equipment, 2.3 Parity DAQ, 2.5 Luminosity Monitor, 2.6 Spectrometers and 2.8 Data Analysis. In the following we will give updates on the beam polarimetry upgrade, changes in the cryo-target cell design, and progress on the fast counting DAQ development.

3.2. Polarimetry

Improvements in polarimetry are of vital importance for the JLab parity violation program. High accuracy (1%) is important not only for this proposal but for the Q_{weak} proposal [E05-

008] [2], PREX [E06-002] [9], PVDIS at 12 GeV [10], and HAPPEX-III [E05-009] [45]. There has been a lot of progress on polarimetry in Hall A in the past two years. Two upgraded polarimeters will be available: The Compton polarimeter and a “high-field” Møller polarimeter, both capable of 1% measurement error in about 1 hour. Our plan is to run the Compton polarimeter continuously and to check periodically with the Møller polarimeter.

The current Compton polarimeter runs well at beam energies ≥ 3 GeV. The Compton has an electron detector and a photon detector, which provide two independent methods of measuring the polarization. These are counting methods, in which electrons or photons are counted in each helicity state and laser polarization state. During the HAPPEX-He experiment the final error achieved was 1.5% with a 3.2 GeV beam. For a 6 GeV beam the error should be smaller, possibly reaching 1%. In addition, the following improvements to the Compton polarimeter have been made or are in progress to achieve a 1% systematic error:

- Some breakthroughs in the analysis of the systematic errors, in particular the parameterization of the response function and the understanding of accidentals, have reduced the systematic error.
- A new integration method is being developed for the photon detector to supplement the two counting methods. Integration will eliminate the systematic errors due to thresholds and deadtime.
- A new photon detector made from a GsO crystal will be made. This will have a high light yield and fast response, thus permitting the integration technique.
- A new green wavelength laser system is being developed. This will improve the figure of merit for low energy electron beams. However, for the purposes of this proposal (6 GeV beam), the old IR laser system would suffice and will be available if necessary.

We expect to achieve 1% by the time PREX and HAPPEX-III run, which could be around the same time as the proposed measurements if they are re-approved.

The Hall A Møller polarimeter is being upgraded. The present Møller polarimeter uses for the target several magnetic foils, tilted at 20° to the beam, magnetized in an external field of about 0.025 T. Measurements are invasive and are done at beam currents below $1 \mu\text{A}$. The systematic

error of about 2% is mainly driven by the uncertainty in the target polarization. It will be reduced to 1% by using the technique of foil saturation developed in Hall C [46], where an iron foil is positioned normally to the beam direction and magnetized along the beam in a field of ~ 4 T. A working magnet exists and is being tested with the new target. This upgrade would allow reduction of the foil polarization error down to about 0.4%, as well as to use a higher beam current of about $3 \mu\text{A}$. The latter improves the accuracy of extrapolation to the regular beam currents of 50 - 100 μA .

3.3. Progress on Target Cell Design

In the original proposal, we used a 25-cm long cryogenic liquid deuterium (LD_2) target with 3 mil Be endcaps. The use of Be endcaps is to minimize the event counts from the endcaps. However it may not be practical to machine thin Be windows at JLab, and we did not specify a detailed design for the target cell.

After discussing with the target group [47], we compared the two available designs of the cry-target cell which may fulfill the requirement of PVDIS: racetrack-shaped (as used in HAPPEX-II) and cylindrical (“cigar-tube”) cells. Racetrack cells have much better cooling flow and thus are usually more suitable for parity experiments, but are in general more difficult to make and the cell window/wall material is limited to certain materials. Cylindrical cells are easier to make and maintain and the up-stream window can be made of special materials like Be. However, it typically have less cooling flow and thus higher boiling noise. To ensure that the measurements will not be affected by boiling noise, we choose to use the racetrack design.

For racetrack cells, the end caps can be made of three possible materials (minimal thicknesses): Be (8.8 mils) (require machining), havar (1.1 mils), and Al 7075-T6 (4.5 mils). Among these, machining the Be is very difficult and will introduce unnecessary health and safety hazard to the laboratory, while havar has poor thermal conductivity (≈ 13 W/Km at room temperature) and is easy to melt in a $85\text{-}\mu\text{A}$ beam. Thus we choose to use 5-mils Al 7075-T6 endcaps. In the following we will analyze event contamination from the new endcaps and the density boiling effects.

3.3.1. Target End Cap Contamination

The endcaps of a typical target cell at JLab are made of ≈ 10 mil aluminum. For $G0$ [48] a special cell was made with Al endcaps ≈ 5 -mils thick. We will use the same endcap thickness as $G0$, and the ratio of yield from endcaps to that from LD_2 is

$$\eta \equiv \frac{N_{endcap}}{N_{LD2}} = \frac{L_{endcap}}{L_{LD2}} \times \frac{\rho_{Al}}{\rho_{LD2}} = \frac{5\text{mils} \times 2}{25\text{cm}} \times \frac{2.7}{0.169} = 1.62\% .$$

This ratio can be measured quickly using an empty target with the same endcaps as the LD_2 cell. Assuming no EMC-like effect, the asymmetry of \vec{e} -Al DIS, A_{Al} , can be calculated as:

$$A_{e-Al} = \left(\frac{3G_F Q^2}{\pi\alpha 2\sqrt{2}} \right) \times \frac{2C_{1u}u_{Al}(x) - C_{1d}[d_{Al}(x) + s_{Al}(x)] + Y[2C_{2u}u_{V,Al}(x) - C_{2d}d_{V,Al}(x)]}{4u_{Al}(x) + d_{Al}(x) + s_{Al}(x)} , \quad (22)$$

where $q_{Al}(x) = Zq^p(x) + Nq^n(x)$ are PDF of aluminum, and $q^p(x)$ and $q^n(x)$ are PDF of the proton and neutron, respectively. Since aluminum has $Z = 13$, $N = 14$, A_{Al} is about 4% different from A_d and will cause a 0.06% effect on the measured value, which is negligible compared to the expected statistical uncertainty. However, there exist no data on \vec{e} -Al DIS asymmetry and to make sure the end-cap correction is under control, the \vec{e} -Al asymmetry, A_{Al} , will be measured using an empty target with thick Al endcaps and the effect on measured A_d will be corrected². The relative uncertainty on A_d due to endcap corrections is

$$\begin{aligned} \frac{\Delta A_{endcap}}{A_d} &= \eta \frac{\Delta A_{Al}}{A_d} = \eta \frac{\Delta A_{Al}}{\Delta A_d} \frac{\Delta A_d}{A_d} = \eta \frac{\sqrt{N_{LD2}}}{\sqrt{N_{Al}}} \frac{\Delta A_d}{A_d} \\ &= \eta \frac{\sqrt{N_{LD2}}}{\sqrt{\lambda N_{endcap}}} \frac{\Delta A_d}{A_d} = \eta \frac{1}{\sqrt{\lambda \eta}} \frac{\Delta A_d}{A_d} = \sqrt{\frac{\eta}{\lambda}} \frac{\Delta A_d}{A_d} = 2\% \sqrt{\frac{1.62\%}{\lambda}} \end{aligned} \quad (23)$$

where λ is the ratio of the product (endcap thickness) \times (production time) of dummy to LD_2 cells. Note that the statistical uncertainty $\Delta A_d = 1/\sqrt{N_{LD2}} \approx 2\% A_d$ was used in the calculation. Limiting $\frac{\Delta A_{endcap}}{A_d} \leq 0.4\%$ we obtain $\lambda > 0.405$. If we match the radiation length of the thick dummy cell to half of the LD_2 , then we need $25 \times$ thicker (3.18 mm) endcaps and up to 1.6% of the beam time will be spent on the dummy production. This means a total of 16 hours will be spent on the dummy cell for the two Q^2 points. The uncertainty on dA_{Al}/A_{Al} will be $\approx 25\%$ for both kinematics.

² This correction will be made only if the measured A_{Al} is different from the expected value.

3.3.2. Boiling Effect

The target boiling effect has two meanings. The first one is the “local boiling effect”, which is the real phase change of the liquid target. We require local boiling to be less than 5% for the proposed measurement. The second meaning is usually used for parity experiments. In this case, “target boiling” is a terminology for (1) the change in target density due to heating of the target, for example, due to deviation in beam parameters, mostly spot size; and (2) pulse-to-pulse target density fluctuation. The latter may cause a false asymmetry and will affect the measurement.

We discuss the second effect first: The measured parity-violating asymmetry of \bar{e} - ^2H scattering is expected to be ≈ 100 ppm. The pulse-to-pulse density fluctuation should be controlled to under 0.05% of this value, *i.e.*, 0.05 ppm. The rate in the Luminosity Monitor is expected to be $> 10^{11}$ Hz per quartz for a 6-GeV beam, therefore it is possible to monitor the false asymmetry to a 100 ppb level ³ within each beam helicity pulse, and hence guarantee the control of the pulse-to-pulse density fluctuation to an acceptable level.

The first effect will generate a non-statistical noise (“boiling noise”) in the signal which is equivalent to an additional statistical fluctuation. The rate for the proposed measurement is around (150 – 500) kHz. The statistical uncertainty per beam pulse pair (33 ms H+ and 33 ms H-, hence total is 66 ms) is on the order of ± 0.01 . To make sure the effect on the measured asymmetry to be negligible, the boiling noise from target should be controlled below 10^{-3} .

In 2004 boiling tests were performed on racetrack-shaped cells [49]. Results suggest a negligible (< 100 ppm) boiling noise at 70 μA current for a 20-cm long LH_2 cell with a 5×5 mm² raster and 60 Hz fan speed. This suggest that racetrack-shaped cell is a much better choice for PVDIS than cigar-tube cell. However, no test was performed on LD_2 cells and we will need to do boiling test before or during the commissioning to optimize the running condition. Suggested starting conditions for the test are 4×4 mm² raster, 60 Hz fan speed, and a current up to 90 μA .

³ Most of the events in Lumi are elastic. The asymmetry is in general proportional to Q^2 , hence the physics asymmetry detected by Lumi is very small, of the order of < 100 ppb. Therefore the false asymmetry can be monitored to ≈ 100 ppb.

3.3.3. Conclusion on Target Design

We choose to use a 25-cm long racetrack-shaped LD₂ cell with 5 mils Al for both entrance and exit windows. A dummy cell is needed with Al endcaps 25× thicker than the LD₂ cell. Boiling tests should be performed before or during the commissioning to study the non-statistical fluctuation of the cell. The suggested test conditions are a raster size of around 4 × 4 mm² (both smaller and bigger sizes will be tested), a fan speed of 60 Hz and a beam current varying from 30 to 90 μA.

3.4. Update on DAQ

In the past year we have solidified our design of the DAQ and have begun the purchasing and assembly, see Fig. 7.

As a reminder, we must use a counting mode DAQ because of the need to separate the pion

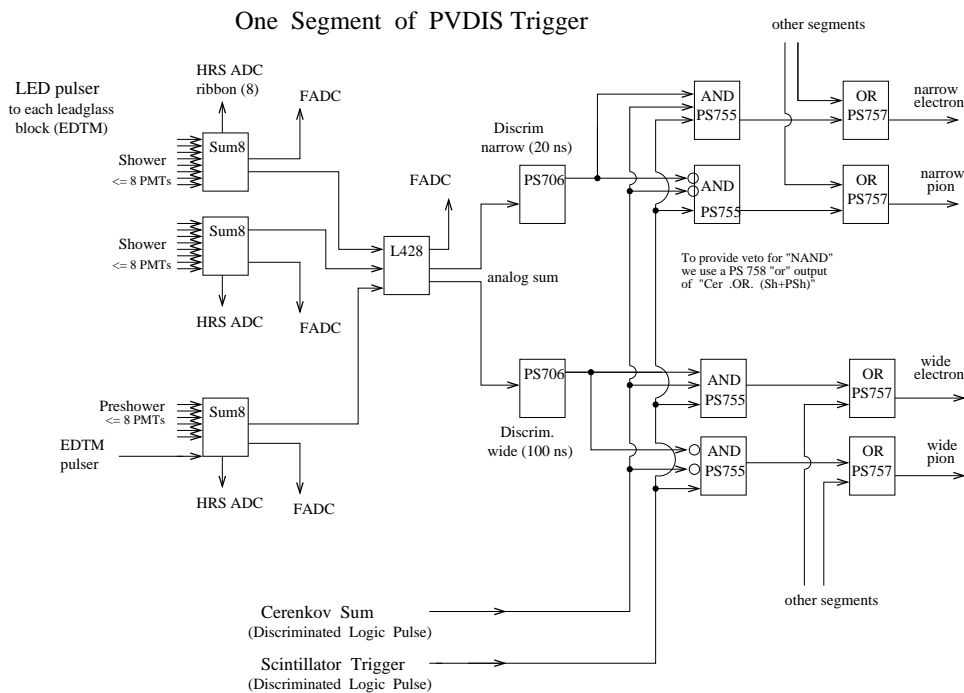


FIG. 7: Schematic layout of PVDIS trigger. The electron and pion triggers (far right) will be counted in scalers gated by helicity. Two discriminator widths are used: a “wide” (100 ns) and a “narrow” (20 ns) width. Comparing the results of these two paths provides a deadtime estimate. The narrow width can be increased if time-walk is a problem, but no larger than 40 ns. See text for detailed explanations.

background. The standard HRS detector signals that we use include the gas Čerenkov detector, two layers of leadglass detectors, and scintillators. Using summing and logic modules, electron and pion triggers are formed and counted in scalars.

The use of scalars to count electrons and pions is a safe, “conventional” approach, but care must be taken to understand deadtime and pileup that will occur at our high rates. While the scaler DAQ is used for production mode, it will be supplemented by FADCs and by the HRS DAQ. The FADCs will be used to study high-rate effects like pileup. The standard HRS DAQ will be used to confirm the trigger logic in low-rate running. We plan on installing this DAQ in the HRS within the next year and testing it parasitically during other experiments. Our goal is to achieve a 1% agreement between the two DAQs.

The electron trigger is the logical “AND” of the leadglass, the Čerenkov detector, and scintillator trigger above thresholds. To avoid missing pulses due to time walk, these signals will be aligned as close as possible using a scope and adjusting with cables. A pion requires a Scintillator trigger and the absence of leadglass and Čerenkov detectors. To form this veto, the leadglass and Čerenkov are “OR”d and fed to a veto input. Summing modules add the signals from groups of 8 leadglass blocks. Experience from RCS and G_N^E experiments show the sum of the whole leadglass detector has too much noise and it is better to sum the blocks in limited regions of the detectors. These trigger regions may share leadglass blocks at their borders to provide good efficiency for showers that straddle the border.

The resulting electron and pion triggers are sent to scalars gated by helicity. This is our “production mode DAQ”: we simply count electrons and pions for each helicity. In addition the triggers are sent to the trigger supervisor to trigger the standard HRS DAQ for a test mode to verify the correctness of the trigger as well as to study backgrounds. Each leadglass block is read in Fastbus ADCs, as well as Čerenkov and scintillators. Therefore, a complete event analysis is possible at low rates. In addition, each sum of leadglass blocks, as well as the summed Čerenkov signal, goes to a FADC to examine pileup.

Measuring the deadtime will be important because the correction to the asymmetry A_d for deadtime δ is $A_d(1 - \delta)$ and since the goal is to measure A_d to 2% the deadtime must be small and known to $\ll 1\%$. The three schemes we are considering to measure deadtime are:

- An LED pulsing system will be deployed for each block of leadglass. The driving pulse can also go to the Čerenkov and scintillator circuits. This is foreseen as an upgrade to the HRS

detector system.

- There are two paths through electronics corresponding to two discriminator widths, a “wide” (100 ns) and a “narrow” (20 ns) width. Comparing the results of these two paths provides a deadtime estimate. The narrow width can be made longer if time-walk turns out to be a problem, but no larger than 40 ns.
- The summing modules have spare inputs into which we will plug a pulser and observe how this gets lost or shifted in time.

As a proof of principle, we have simulated the PVDIS trigger using real data from a completed DIS experiment (e99117) that ran in Hall A which had a large fraction of pions ($\frac{\pi}{e} \sim 23$). The data from that experiment are sent through an algorithm which simulates the proposed trigger electronics. The Čerenkov is summed and a cut applied to identify electron candidates. The leadglass is summed in regional groups to simulate the summing modules and a cut (discriminator threshold) is applied to the group. In the real experiment gains will be matched and the discriminator thresholds will be determined before the start of the experiment from ADC spectra. This trigger simulation studied the electron detection efficiency, pion rejection efficiency, and backgrounds. It also studied the need for overlapping the leadglass regions. We found a 99% electron efficiency and a 10^3 pion rejection, both of which are acceptable. We also found a 2% background which have no track pointing back to the target yet satisfy the electron trigger, which is probably caused by scattering of electrons in the stainless steel vacuum box at the exit of the spectrometer (Q3), as has been seen in other experiments. However the kinematics of these events should be very close to those pass through the spectrometer and the effect on the measured asymmetry is thus very small. We’ll need to do auxiliary low-rate measurements with the standard HRS DAQ to study this background; these could include scans of the HRS dipole, empty-target runs, and runs with extra collimation. More discussion on background can be found in section 4.3.

3.5. Overview of Instrumentation

TABLE III: An overview of instrumentation for the proposed measurement.

Instrument	Components and status	Need special development?
Beam polarimeter	<ul style="list-style-type: none"> • Compton green laser and electron detector upgrade; • Compton photon integration method as a cross-check of the electron method; • Møller upgrade planned for PREX <p><i>(All are being developed and will be used for PREX)</i></p>	<p>Yes</p> <p>Yes</p> <p>Yes</p>
Beam line	<ul style="list-style-type: none"> • Standard ARC and eP 	
Beam Helicity Control	<ul style="list-style-type: none"> • Parity DAQ and helicity feedback 	
Luminosity Monitor	<ul style="list-style-type: none"> • Well developed, used for HAPPEX II, will be used for PREX and HAPPEX III 	
Cryogenic Target	<ul style="list-style-type: none"> • 25-cm long tracktrack LD2 target with 5 mil Al end-windows, maximum Hall A target cooling power needed; 	<p>Yes, need new cell and boiling test</p>
Spectrometers	<ul style="list-style-type: none"> • Two HRS taking data simultaneously 	
DAQ	<ul style="list-style-type: none"> • A fast counting, scaler-based DAQ <i>(parts ordered, being assembled)</i> • A modified FADC system <i>(currently being designed by the electronics group as part of the 12 GeV upgrade, prototype available soon; commercial units also available.)</i> 	<p>Yes, parasitic testing expected</p>
PID Detectors	<ul style="list-style-type: none"> • Scintillator counters; gas Čerenkov counter, double-layered Pb glass shower counter. Pion rej. $> 10^4$ with regular DAQ (well established) and $> 10^3$ with fast counting DAQ 	<p>Need DAQ test</p>

4. UPDATES ON EXPECTED UNCERTAINTIES AND RATE ESTIMATION

In this section we give an update on the systematic uncertainties for A_d and theoretical uncertainties for extracting $(2C_{2u} - C_{2d})$. Then we give the updated rate estimate and beam time request.

Compared to the original proposal, no change has been made to the uncertainties related to: deadtime correction, target purity, target density fluctuation and other false asymmetries; pion background, pair production background, experimental uncertainties (Q^2 and the acceptance), electroweak radiative corrections, and the method for kinematics optimization. These were described in Sections 3.1, 3.2, 3.4, 3.5, 3.7, 3.8 and 3.11 of the original proposal. We will update below changes in the target end cap contamination, rescattering background, and electromagnetic radiative corrections.

One major change here is how we deal with some of the poorly understood hadronic uncertainties, namely higher twists (HT) and charge symmetry violation (CSV) effects. In the original proposal we have included the uncertainties due to HT and CSV in the systematic uncertainty for $(2C_{2u} - C_{2d})$. However, these hadronic effects are calculated only from models or global fits obtained from indirect measurements, which could be unreliable and do not provide definite constraints on how large they could be for the proposed kinematics. Furthermore, the goal of this proposed measurement at 6 GeV is not to precisely separate the electroweak and the hadronic effects, but rather to measure A_d to a high precision and to investigate whether these effects are significant. Therefore in this update, we will only provide HT and CSV uncertainties on A_d from the latest calculations and global fits, and the resulting uncertainties on $2C_{2u} - C_{2d}$, but do not include them in the total uncertainties on $2C_{2u} - C_{2d}$.

4.1. Target End Cap Contamination

The target cell are made of 10 mil Al walls with 5 mil Al in the central region of both endcaps. As discussed in Section 3.3, we will measure the \vec{e} -Al PVDIS asymmetry such that the overall uncertainty on A_d due to endcaps is controlled to below 0.4%. Although from PVDIS models we expect that effect from the endcaps to A_d to be much less than this level, we will use 0.4% for systematic uncertainty estimate for A_d here. The endcaps of dummy cell will be 25 times thicker than the LD₂ cell, and we will spend 1.62% of the LD₂ production time on the dummy cell.

4.2. Electromagnetic (EM) Radiative Correction

Figure 1 describes the scattering process at tree level. In reality both the incident and the scattered electrons can emit photons, and the kinematics (Q^2 , W) at the reaction vertex differ from that reconstructed from the measured momentum and angle of the scattered electron. Consequently when we extract cross sections and asymmetries from the measured values there are electromagnetic radiative corrections to be made. The theory for the EM radiative correction is well developed [50] and the correction can in principle be calculated. However the uncertainty of this correction depends largely on the uncertainty of the input structure functions and parity violating observables. For our proposed kinematics, the difference between the vertex and the reconstructed kinematics is located partly in the nucleon resonance region. On the other hand, PV asymmetries in the resonance region are not well known, except some limited data for the $\Delta(1232)$. In principle, if duality works then the effect from resonance structures would be small and one can use DIS formula to calculate the PV asymmetries needed for the radiative correction. But we do not know yet if duality works in PV processes. To limit the uncertainty of EM radiative corrections to a tolerable level, we plan to measure the PV asymmetry in the relevant resonance region.

Figure 8 shows the vertex kinematics for the two proposed DIS measurements at $Q^2 = 1.11$ (left) and 1.90 (GeV/c)² (right). The red spectrum show the reconstructed (measured) Q^2 and W without radiative effects and the green spectrum show the vertex Q^2 and W values. For each kinematics, about (15-18)% of events will come from resonance regions due to internal and external bremsstrahlung. To limit the contribution to the uncertainty on A_d from electromagnetic radiative correction to less than 1%, we will measure the resonance PV asymmetry to $dA_{res}/A_{res} < 5\%$ and $< 8\%$ for the $Q^2 = 1.11$ and 1.90 (GeV/c)² points, respectively (here the slightly different goal comes from the difference between the expected asymmetry in the resonance region, A_{res} , and the value of A_d at the two DIS kinematics). Also shown in Fig. 8 are the Q^2 and W coverages for the five resonance measurements. The beam energies are 4.8 and 6.0 GeV. Results of these measurements can be interpolated in Q^2 to cover the full kinematic region needed for radiative corrections for the two DIS measurement. Table IV shows the kinematics, expected asymmetry, rates and estimated beam time for these measurements. We use 1% for the uncertainty on A_d due to the resonance structure in EM radiative corrections.

FIG. 8: Kinematic coverage for the two DIS and the five (#3-#7) resonance measurements. Kinematics #1 and #2 are for the two DIS measurements at $Q^2 = 1.1$ and 1.9 $(\text{GeV}/c)^2$, respectively.

PVDIS at 6 GeV Simulation

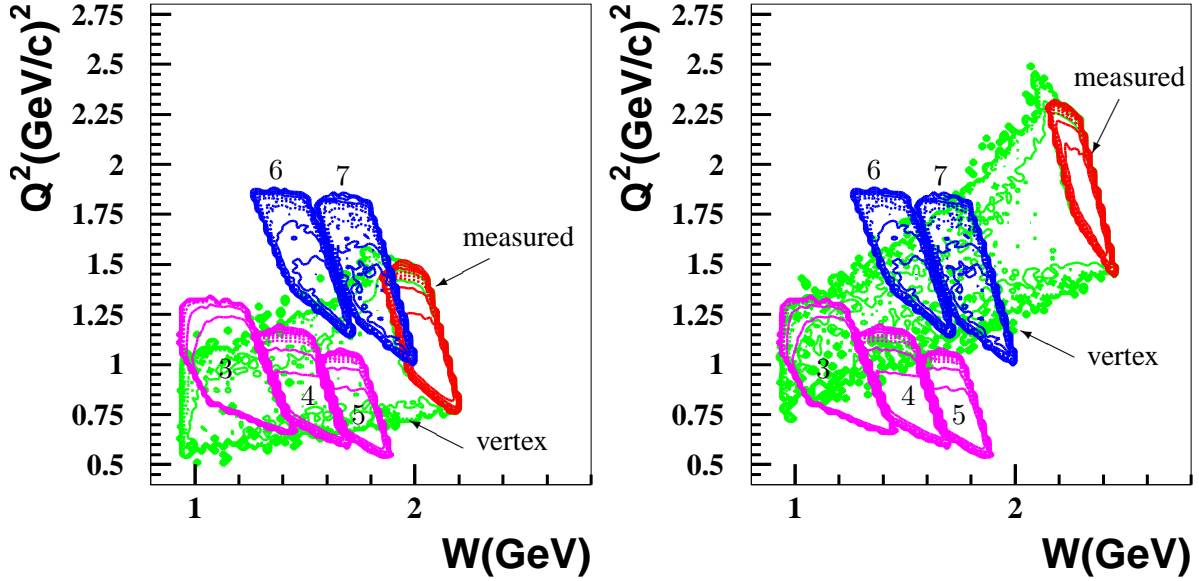


TABLE IV: Kinematics for resonance measurements. Rates and beam times are for **one** HRS. The π^- and e^+ rates are from Wiser's fit which is known to overestimate in the resonance region. The asymmetries are calculated using the DIS formula. The beam time estimation is for single HRS and has taken into account the 80% beam polarization. The total beam time needed is 95 hours for two HRSs, or 4 days.

Kinematics	E (GeV)	θ θ	E' (GeV)	$\langle Q^2 \rangle$ $(\text{GeV}/c)^2$	$\langle W \rangle$ (GeV)	e^- rate (KHz)	π^- rate (KHz)	e^+ rate (Hz)	A_d (ppm)	goal for $\Delta A_d/A_d$	Beam time (hours)
3	4.8	12.9°	4.00	0.92	1.22	983.0	2.0	0.62	-72.4	5%	33.7
4	4.8	12.9°	3.60	0.85	1.51	915.1	15.8	11.85	-68.4	5%	40.5
5	4.8	12.9°	3.25	0.77	1.74	833.7	48.9	62.79	-63.0	5%	52.5
6	4.8	19.0°	2.77	1.49	1.52	104.5	3.6	2.2	-120.7	8%	44.6
7	6.0	14.0°	4.00	1.39	1.80	279.7	11.2	10.0	-113.0	8%	19.0

4.3. Rescattering Background

The rescattering of high-energy electrons or pions from the walls of the spectrometer creates a potential source of background for the proposed measurement. This “rescattering” background, which is typically rejected using a combination of tracking and particle identification in low-rate experiments without difficulty, must be treated carefully in this high-rate measurement due to the limited information available in each event.

The magnitude of this effect will be combination of the probability for products of this scattering in the spectrometer to reach the detectors and the effectiveness of the detector/DAQ package to distinguish those tracks from tracks originating in the target. A detailed analysis of this possible problem will require a careful simulation of the spectrometer and detector geometry. Measurements will be taken with a low beam current (to allow the use of the tracking chambers and the standard DAQ) to study this small background and verify the accuracy of the simulation.

Rescattering contribution has been studied by the previous HAPPEX II experiments in Hall A (HAPPEX-H: E99-115 and HAPPEX-He: E00-114) [51]. These experiments used an analog-integrating detector, and therefore had no method for excluding rescattered background particles. The method used includes a series of dedicated elastic scattering measurements with a hydrogen target, with the spectrometer tuned to place the hydrogen elastic peak at various points inside the spectrometer. The detected rate was used to estimate the “rescattering probability”: the probability that an electron, interacting at a given point in the spectrometer, produces a count in the production DAQ. In those measurements, the rescattering probability was found to be around 1% for momenta near to the central momenta (within a few percent of $\delta p/p$). This probability rapidly dropped to 10^{-5} for interactions with the spectrometer wall took place before the last spectrometer quadrupole element (Q3). For HAPPEX-He, the rate of quasi-elastic scattering from the Helium target which was steered into the spectrometer walls was several times the elastic signal rate, leading to a rescattering in the focal plane on order 0.2% of the detected elastic rate. It is reasonable to expect that the detected rescattering signal in the proposed measurement will also form a dilution at the few 10^{-3} level. Factors that would argue for a larger contribution, such as the continuous DIS momentum distribution and the relatively open spectrometer geometry, will be counteracted by the ability to exclude background through position, energy, or PID information from the fast counting DAQ.

One also have background from pion rescattering. However, pions can be rejected by PID

detectors reliably and will only have negligible contribution to the primary measurement.

Overall, we expect that the total rescattering rate to be at most at a few $\times 10^{-3}$ level. And among these rescattered events, resonance electrons and pions will only consist a small fraction. The rescattered DIS electrons may be the majority of these rescattering events but they have very similar kinematics and Q^2 to the primary measurement thus will only introduce a very small dilution. Therefore we expect the total uncertainty due to the rescattered background to be in the 10^{-4} range.

4.4. Parton Distribution Functions and Ratio R

For R we used the same fit (R1998) [52] as in the original proposal. But we have corrected a mistake in the code and have updated the uncertainty due to R . For the parton distribution functions, in the original proposal we used MRST2001E [53] and CTEQ6M [54]. Here we have updated the MRST results using their latest fit with uncertainties, MRST2006nnlo [55], and found the difference in A_d between the two MRST versions is very small, $< 0.2\%$. The difference between MRST2006nnlo and CTEQ6M is $< 0.3\%$. Using a similar method as in the original proposal, we used the A_d uncertainties calculated from each PDF set as well as the difference between them to estimate the uncertainty in the extracted $(2C_{2u} - C_{2d})$. The effects are found to be $\Delta(2C_{2u} - C_{2d}) = 0.0071$ and 0.0031 for the low and high Q^2 point, respectively.

4.5. Higher Twists Effects

In Section 2.2.1 we have reviewed the current status of theories and data on higher-twist (HT) effects. Most of these available theories or phenomenological fits predict that the HT contribution to A_d is at the $1\%/Q^2$ level. And we will summarize these predictions in table VIII. However, there has been no direct measurement of HT contribution to PV observables and we do not know how reliable these predictions are. That is the main reason why we propose two kinematics, because the lower Q^2 kinematics would show almost twice as large HT effects as the higher Q^2 point.

Since our submission of the original proposal, status on HT theory has not changed much. This is partly because there exist no parity violating data to refine theories. On the other hand, we have full support from theorists should this proposal be approved again, and will likely have QCD-based HT calculations available in the near future.

4.6. Charge Symmetry Violation (CSV)

Recent advances in the understanding of CSV are discussed in Sec. 2.2.2. Different splitting functions for the u and d quarks provide for different DGLAP evolution [41, 42, 43]. This effect has now been included in the parton distributions. There is additionally a possibility of an anomalous, hadronic CSV. The combination of this and QED CSV was parameterized by MRST in a recent global parton distribution fit [35] which examined theoretical assumptions used in these fits. MRST found that the χ^2 minimum preferred a small violation of CSV. However based on the 90% CL limits of this fit, an effect from CSV could be as large as half of the statistical uncertainty of the proposed measurement. Calculations for CSV for the proposed kinematics will be summarized in Table VIII and IX.

4.7. Rate Estimation and Kinematics Optimization

The updated kinematics and rates are shown in Table V. The kinematics are the same as in the original proposal. The optimization of the two kinematics were demonstrated in the original proposal and will not be repeated here. For DIS rates we used the NMC95 unpolarized DIS fit [56]. Pion and positron (pair production) rates are estimated using Wiser's [57] fit and the known π^0 decay properties, then multiplied by 2 for conservative estimates. The radiation length before interaction is needed for both pion and positron rate estimations, and the radiation length after interaction is needed for positrons. The slight difference in positron rates, compared to our original proposal, comes from a more accurate model for the target cell geometry, wall thickness, and the spectrometer entrance windows.

4.8. Error Budget

Expected experimental and theoretical uncertainties on the asymmetry A_d are shown in Table VI and VII, respectively. Estimation for higher twist and CSV uncertainties on A_d are shown in Table VIII. Expected uncertainties on $2C'_{2u} - C'_{2d}$ extracted from A_d are shown in Table IX, which include A_d uncertainties in Table VI and VII, but not higher twist and CSV uncertainties.

TABLE V: Kinematics for the Proposed Measurements. Rates are for **each** HRS and π^-/e^- ratios are two times results from Wisner's fit. Due to limitations on the HRS momentum settings, the low Q^2 measurement will take place on the left HRS and the high Q^2 measurement will be shared by the two HRSs.

Kinematics	I	II
x_{Bj}	0.25	0.30
Q^2 (GeV/c) ²	1.11	1.90
E (GeV)	6.0	6.0
E' (GeV)	3.66	2.63
θ	12.9°	20.0°
W^2 (GeV) ²	4.16	5.30
Y	0.470	0.716
R_c	< 0.001	0.001
R_s	0.052	0.041
R_v	0.872	0.910
A_d (measured, ppm)	-91.3	-160.7
e^- rate (KHz)	269.8	25.1
π^-/e^- ratio	0.9	6.4
e^+/e^- ratio	0.073%	0.463%
total rate (KHz)	513.0	186.2
e^- production time (days)	9.0	32.0
dummy cell (endcap) runs (hours)	3.5	12.4
e^+ runs (hours)	4.0	4.0

TABLE VI: Expected uncertainties on the asymmetry A_d . The systematic uncertainties are the same for both Q^2 points. Numbers shown are for $\Delta A_d/A_d$.

Source		$Q^2 = 1.11 \text{ (GeV}/c)^2$	$Q^2 = 1.90 \text{ (GeV}/c)^2$
Systematics	$\Delta P_{beam}/P_{beam} = 1\%$	1%	1%
	Deadtime correction	$\approx 0.3\%$	$\approx 0.3\%$
	Event pile-up	$\approx 0.1\%$	$\approx 0.1\%$
	Target endcap contamination	0.4%	0.4%
	Target density	0.1%	0.1%
	Target purity	$< 0.02\%$	$< 0.02\%$
	Pion background	$< 0.2\%$	$< 0.2\%$
	Pair production background	$< 0.2\%$	$< 0.2\%$
	Total syst.	1.36%	1.36%
Statistical		2.11%	2.09%
Total	Syst.+Stat.	2.52%	2.49%

TABLE VII: Theoretical uncertainties on the asymmetry A_d used in the extraction of $2C_{2u} - C_{2d}$. Numbers shown are for $\Delta A_d/A_d$.

Source		$Q^2 = 1.11 \text{ (GeV}/c)^2$	$Q^2 = 1.90 \text{ (GeV}/c)^2$
Theoretical	Q^2	0.18%	0.12%
	$R = \sigma_L/\sigma_T$	0.0036%	0.0110%
	PDF uncertainties	0.33%	0.25%
	EM radiative corrections	0.4%	0.4%
	EW radiative corrections	0.2%	0.2%
	Total	1.09%	1.06%

TABLE VIII: Estimation for higher twist and CSV effects on the asymmetry. Numbers shown are $\Delta A_d/A_d$. These are not included in the final uncertainty of $2C_{2u} - C_{2d}$.

Source		$Q^2 = 1.11 \text{ (GeV/c)}^2$	$Q^2 = 1.90 \text{ (GeV/c)}^2$
HT effects	MIT bag model I [36]	0.3%	0.15%
	MIT bag model II [37]	$< 2\%/Q^2$	$< 2\%/Q^2$
	Calculation using C_{HT} fits [38] from $F_{1,2}$ data [34]	$< 1\%/Q^2$ (for $0.1 < x < 0.3$)	$< 1\%/Q^2$ (for $0.1 < x < 0.3$)
Hadronic CSV	valence (nominal) (90% C.L.)	0.053% (0.214%, -0.175%)	0.085% (0.339%, -0.273%)
	sea (nominal) (90% C.L.)	-0.303% (0.305%, -0.677%)	-0.224% (0.227%, -0.503%)
	total (nominal)	-0.250%	-0.140%
	(90% C.L.)	(0.522%, -0.848%)	(0.567%, -0.773%)

TABLE IX: Expected uncertainty on $2C_{2u} - C_{2d}$. Uncertainties due to higher-twist and CSV effects are shown but are not included in the total uncertainty.

Source/ $\Delta(2C_{2u} - C_{2d})$	$Q^2 = 1.11 \text{ (GeV/c)}^2$	$Q^2 = 1.90 \text{ (GeV/c)}^2$
Statistical (from A_d)	0.0399	0.0253
Systematics (from A_d)	0.0257	0.0165
Experimental (Q^2)	0.0040	0.0017
$\Delta R \equiv \sigma_L/\sigma_T$	0.00006	0.00013
Parton Distributions	0.0071	0.0031
Electro-magnetic Radiative Correction	0.0189	0.0121
Electro-weak Radiative Correction	0.0038	0.0024
Higher Twist Effect (using $1\%/Q^2$ on A_d)	0.0170	0.0064
Charge Symmetry Violation (nominal)	0.0054	0.0031
Charge Symmetry Violation (90% C.L.)	0.0132	0.0085
total uncertainty (excluding HT and CSV)	0.0518	0.0329

5. BEAM TIME REQUEST

We request 50 days of beam time for measurements of $\Delta_{\text{stat}} A_d/A_d = 2\%$ at two Q^2 values. If the higher twist contribution measured to be small, the expected precision on the C_{2q} result is $\Delta(2C_{2u} - C_{2d}) = 0.033$. Within these 50 days, 42.0 days are for DIS production running, including 41.0 days for e^- runs, 8.0 hours for e^+ runs and 15.9 hours for measuring the asymmetry of dummy cell Al end caps. Resonance measurement takes 4.0 days. We need four days for commissioning of the fast counting DAQ system and the Compton polarimeter, and measuring Q^2 and checking PID performance with the regular counting DAQ as well as the fast counting DAQ. Table X summarizes the details of the proposed measurements. Beam times are given in “two-HRS equivalent”. For example, electron production data for $Q^2 = 1.11 \text{ (GeV}/c)^2$ will be collected on the HRS-L within $2 \times 9.0 = 18$ days, meanwhile the HRS-R is used to collect data for $Q^2 = 1.90 \text{ (GeV}/c)^2$. Then both HRS will be collecting data for $Q^2 = 1.90 \text{ (GeV}/c)^2$ simultaneously for $32 - 9 = 23$ days.

TABLE X: Kinematics and estimated running time given in “two-HRS equivalent” (see text for details). Beam times needed for resonance measurement and commissioning (four days) are not listed here. Details of the resonance measurement can be found in Section 4.2.

E_b (GeV)	θ	E_p (GeV)	Q^2 (GeV/c) ²	e^- production (days)	e^+ run (hours)	dummy (hours)	total beam time (days)
6.0	12.9°	3.66	1.11	9.0	4.0	3.5	9.3
6.0	20.0°	2.63	1.90	32.0	4.0	12.4	32.7

In the original proposal we have divided the running into two phases, where only phase I (13 days) was approved by PAC 27. **To achieve the greatest scientific impact, we request here approval for the full 50 days.** In the event that less beam time is available, the impact on the physics-based goals of the experiment has been evaluated. This impact is given in Tab. XI in terms of the expected total uncertainty on A_d and $2C_{2u} - C_{2d}$, as well as the factor of improvement on $2C_{2u} - C_{2d}$ compared to the current PDG value best fit.

TABLE XI: Physics outcome from full and partial running. Production times (given for two HRS's) include dummy cell and e^+ runs. The total beam times include the resonance measurement and the 4-day commissioning.

Production time (days) $Q^2 = 1.1$	Production time (days) $Q^2 = 1.9$	Production time (days) resonances	$\Delta A_d/A_d$ ($Q^2 = 1.11$)	$\Delta A_d/A_d$ ($Q^2 = 1.90$)	$\Delta(2C_{2u} - C_{2d})$ ($Q^2 = 1.90$)	factor of improvement on $(2C_{2u} - C_{2d})$	total beam time needed
9.3	32.7	4.1	2.52%	2.49%	0.0329	5.9	50 days
7.5	26.3	3.3	2.72%	2.70%	0.035	5.5	41 days
5.6	19.6	2.8	3.06%	3.02%	0.039	5.0	32 days

6. COLLABORATION STATUS

There have been several changes to the collaboration since the approval of the original proposal. Robert Michaels from Hall A has joined the experiment as a co-spokesperson after its approval in 2005. Ramesh Subedi has joined Univ. of Virginia as a postdoctoral researcher in Nov. 2007 and his main responsibility is to prepare the running of E05-007, focusing on the design, assembly and testing of the new counting DAQ. We also have 2 or 3 first-year graduate students interested in doing Ph.D. on this experiment: Xiao-Yan Deng, Dian-cheng Wang (Univ. of Virginia), and Jin Huang (MIT). All three are planning to be stationed at JLab starting January or June 2008. We hope the experiment can be fully approved and run in 2009 so these young physicists can collect their thesis data on time.

7. RELATION TO OTHER JLAB EXPERIMENTS AND THE 12 GEV ELECTROWEAK PHYSICS PROGRAM

Testing the electroweak Standard Model is the goal of many low- and medium-energy experiments: atomic parity violation (APV) on Ti and Cs, PV in Møller scattering (SLAC E158), the NuTeV experiment at FNAL, the Qweak experiment to run in JLab Hall C, and the future electroweak physics program at the upgraded 12 GeV JLab. The PVDIS measurement proposed here is

complementary to these experimental searches because PVDIS is the only process that can access the C_{2q} couplings, and thus the quark axial couplings. For example, the Møller experiment is based on a purely leptonic process and cannot access the quark sector of the SM; the APV and the future Qweak experiments are only sensitive to C_{1q} , though Qweak will provide the most precise data on these couplings. In the following we discuss how the proposed measurements are related to the 12 GeV electroweak physics program at JLab.

The discussion on how the upgraded 12 GeV JLab can contribute to our understanding of electroweak physics has been focused on two programs: measurement of the PV asymmetry in Møller scattering, and measurement of the PVDIS asymmetry, both to higher precisions than what have been achieved at SLAC or will be achieved with the 6 GeV beam. The Møller experiment, again, is purely leptonic and cannot provide information on new physics in the quark sector, thus is complementary to the PVDIS program at both 6 and 12 GeV. Measurement of the PVDIS asymmetry on deuterium using baseline equipment in Hall C was proposed to PAC32. It will measure A_d at $Q^2 \approx 3 \text{ (GeV}/c)^2$, and was conditionally approved because of challenges in both experimental technique and theoretical interpretations [10], in particular we do not know how large the higher twist effects could be. It is also possible to measure PVDIS asymmetries using a large acceptance, dedicated device, which is being discussed by the electroweak collaboration and will be proposed soon to the 12 GeV PAC. This new device will allow a detailed mapping of A_d at different (x, Q^2, y) , and will allow a good separation of the higher twist, CSV, and beyond the SM effects. **To evaluate the likelihood of success for these 12 GeV PVDIS programs, it is critical to know the size of higher twist effect. This information will be provided by measurement from this experiment.** Clearly, results from the measurement proposed here will provide valuable guidance to the 12 GeV PVDIS program, no matter which approach will be chosen in the future.

8. SUMMARY

We propose to measure the parity violating asymmetry A_d for \vec{e}^- - ^2H deep inelastic scattering at two Q^2 values and $x = 0.25 \sim 0.30$ using a 25-cm liquid deuterium target in Hall A and an 85- μA polarized beam. Assuming an 80% beam polarization, we request 50 days of total beam time to reach a total (statistical) uncertainties of $\Delta A_d/A_d = 2.52\%(2.11\%)$ and $2.49\%(2.09\%)$ at $Q^2 = 1.11$ and $1.90 \text{ (GeV}/c)^2$, respectively. If the higher twist effects are found to be small, the

uncertainty on the effective coupling constant is expected to be $\Delta(2C_{2u} - C_{2d}) = 0.033$. Among these 50 days, 13 days were approved by PAC 27 and rated A-, and are now under jeopardy review. We request here full approval—50 days—of the proposed measurement.

The proposed measurement is the first step of the PVDIS program at JLab. The expected precision *of this measurement* on $2C_{2u} - C_{2d}$ will improve the current knowledge on this quantity by a factor of six. The result will help to extract C_{3q} from high energy data, and has the potential to reveal possible new physics beyond the Standard Model. The higher-twist effects explored by the low Q^2 measurement will provide the first, crucial guidance on the interpretation of existing data and on the future PVDIS measurements at the JLab 12 GeV upgrade.

Acknowledgment

We would like to thank Michael Ramsey-Musolf for useful discussions.

- [1] P. L. Anthony et al. (SLAC E158), Phys. Rev. Lett. **95**, 081601 (2005), hep-ex/0504049.
- [2] R. Carlini, J. M. Finn, S. Kowalski, S. Page, et al., *The Q_{weak} experiment: A search for new physics at the tev scale via a measurement of the proton's weak charge* (2001), JLab E02-020.
- [3] D. S. Armstrong et al. (G0), Phys. Rev. Lett. **95**, 092001 (2005), nucl-ex/0506021.
- [4] A. Acha et al. (HAPPEX), Phys. Rev. Lett. **98**, 032301 (2007), nucl-ex/0609002.
- [5] K. A. Aniol et al. (HAPPEX), Phys. Lett. **B635**, 275 (2006), nucl-ex/0506011.
- [6] K. A. Aniol et al. (HAPPEX), Phys. Rev. Lett. **96**, 022003 (2006), nucl-ex/0506010.
- [7] F. E. Maas et al., Phys. Rev. Lett. **94**, 152001 (2005), nucl-ex/0412030.
- [8] F. E. Maas et al. (A4), Phys. Rev. Lett. **93**, 022002 (2004), nucl-ex/0401019.
- [9] R. Michaels, P. Souder, G. Urciuoli, et al., *A clean measurement of the neutron skin of ^{208}Pb through parity violating electron scattering* (2005), JLab E06-002.
- [10] K. Paschke, P. Reimer, X.-C. Zheng, et al., *Precision measurement of the parity-violating asymmetry in deep inelastic scattering off deuterium using baseline 12 GeV equipment in Hall C* (2007), JLab 12 GeV PR12-07-102.
- [11] P. A. Souder, AIP Conf. Proc. **747**, 199 (2005).
- [12] R. N. Cahn and F. J. Gilman, Phys. Rev. **D17**, 1313 (1978).
- [13] P. Bosted et al. (SLAC E149 Collaboration), *DIS-Parity: Parity violation in deep-inelastic electron scattering* (1993), SLAC Proposal E-149.
- [14] S. C. Bennett and C. E. Wieman, Phys. Rev. Lett. **82**, 2484 (1999), hep-ex/9903022.
- [15] P. A. Vetter, D. M. Meekhof, P. K. Majumder, S. K. Lamoreaux, and E. N. Fortson, Phys. Rev. Lett. **74**, 2658 (1995).
- [16] A. I. Milstein, O. P. Sushkov, and I. S. Terekhov, Phys. Rev. Lett. **89**, 283003 (2002), hep-ph/0208227.
- [17] R. D. Young, R. D. Carlini, A. W. Thomas, and J. Roche, Phys. Rev. Lett. **99**, 122003 (2007), arXiv:0704.2618 [hep-ph].
- [18] C. Y. Prescott et al., Phys. Lett. **B77**, 347 (1978).
- [19] C. Y. Prescott et al., Phys. Lett. **B84**, 524 (1979).

- [20] M. J. Ramsey-Musolf, Phys. Rev. **C60**, 015501 (1999), hep-ph/9903264.
- [21] J. Erler and M. J. Ramsey-Musolf, Phys. Rev. **D72**, 073003 (2005), hep-ph/0409169.
- [22] W. M. Yao et al. (Particle Data Group), J. Phys. **G33**, 1 (2006).
- [23] J. Erler and M. J. Ramsey-Musolf, Prog. Part. Nucl. Phys. **54**, 351 (2005), hep-ph/0404291.
- [24] P. A. Souder et al., Phys. Rev. Lett. **65**, 694 (1990).
- [25] E. J. Beise, M. L. Pitt, and D. T. Spayde, Prog. Part. Nucl. Phys. **54**, 289 (2005), nucl-ex/0412054.
- [26] R. Young (2007), private Communication.
- [27] A. Argento et al., Phys. Lett. **B120**, 245 (1983).
- [28] T. M. Ito et al. (SAMPLE), Phys. Rev. Lett. **92**, 102003 (2004), nucl-ex/0310001.
- [29] D. T. Spayde et al. (SAMPLE), Phys. Lett. **B583**, 79 (2004), nucl-ex/0312016.
- [30] P. L. Anthony et al. (SLAC E158), Phys. Rev. Lett. **92**, 181602 (2004), hep-ex/0312035.
- [31] G. P. Zeller et al. (NuTeV), Phys. Rev. Lett. **88**, 091802 (2002), hep-ex/0110059.
- [32] D. Mason et al. (NuTeV), Phys. Rev. Lett. **99**, 192001 (2007).
- [33] M. Gluck and E. Reya, Phys. Rev. Lett. **47**, 1104 (1981).
- [34] M. Virchaux and A. Milsztajn, Phys. Lett. **B274**, 221 (1992).
- [35] A. D. Martin, R. G. Roberts, W. J. Stirling, and R. S. Thorne, Eur. Phys. J. **C35**, 325 (2004), hep-ph/0308087.
- [36] P. Castorina and P. J. Mulders, Phys. Rev. **D31**, 2760 (1985).
- [37] S. Fajfer and R. J. Oakes, Phys. Rev. **D30**, 1585 (1984).
- [38] W. V. Neerven (2003), private Communication.
- [39] G. A. Miller, B. M. K. Nefkens, and I. Slaus, Phys. Rept. **194**, 1 (1990).
- [40] J. T. Londergan and A. W. Thomas, Phys. Lett. **B558**, 132 (2003), hep-ph/0301147.
- [41] A. Vogt, S. Moch, and J. A. M. Vermaseren, Nucl. Phys. **B691**, 129 (2004), hep-ph/0404111.
- [42] S. Moch, J. A. M. Vermaseren, and A. Vogt, Nucl. Phys. **B688**, 101 (2004), hep-ph/0403192.
- [43] A. D. Martin, R. G. Roberts, W. J. Stirling, and R. S. Thorne, Eur. Phys. J. **C39**, 155 (2005), hep-ph/0411040.
- [44] E. Sather, Phys. Lett. **B274**, 433 (1992).
- [45] K. Paschke, P. Souder, et al., *A measurement of neutron strange form factors at high q^2* (2005), JLab E05-109.
- [46] M. Hauger et al., Nucl. Instrum. Meth. **A462**, 382 (2001), nucl-ex/9910013.

- [47] D. Meekins (2005), this section is based on Dave Meekins presentation at the collaboration meeting on February 17, 2005.
- [48] D. Beck et al., *G0 experiment: Forward and backward angle measurements* (2000 and 2006), JLab E00-006 and E06-008.
- [49] D. Armstrong (2005), presentation at the HAPPEX collaboration meeting on February 18, 2005. <http://hallaweb.jlab.org/experiment/HAPPEX/minutes/05Feb18/>.
- [50] L. W. Mo and Y.-S. Tsai, *Rev. Mod. Phys.* **41**, 205 (1969).
- [51] *HAPPEX-H (E99-115) and HAPPEX-He (E00-114) experiments* (2005), URL <http://hallaweb.jlab.org/experiment/HAPPEX/>.
- [52] K. Abe et al. (E143), *Phys. Lett.* **B452**, 194 (1999), hep-ex/9808028.
- [53] A. D. Martin, R. G. Roberts, W. J. Stirling, and R. S. Thorne, *Eur. Phys. J.* **C28**, 455 (2003), hep-ph/0211080.
- [54] J. Pumplin et al., *JHEP* **07**, 012 (2002), hep-ph/0201195.
- [55] A. D. Martin, W. J. Stirling, R. S. Thorne, and G. Watt, *Phys. Lett.* **B652**, 292 (2007), arXiv:0706.0459 [hep-ph].
- [56] M. Arneodo et al. (New Muon.), *Phys. Lett.* **B364**, 107 (1995), hep-ph/9509406.
- [57] D. E. Wisner, Ph.D. thesis, University of Wisconsin (1977), UMI 77-19743.